Correlations among carbohydrate inventories, enzyme activities, and microbial communities in the western North Atlantic Ocean

C. Chad Lloyd[1], Sarah Brown[2], Greta Giljan[3], Sherif Ghobrial[1], Silvia Vidal-Melgosa[3,4], Nicola Steinke[3], Jan-Hendrik Hehemann[3,4], Rudolf Amann[3], Carol Arnosti[1]

5 [1]Department of Earth, Marine and Environmental Sciences, University of North Carolina at Chapel Hill, Chapel Hill, 27599, USA
[2]Environment, Ecology, and Energy Program, University of North Carolina at Chapel Hill, Chapel Hill, 27599, USA
[3]Max Planck Institute for Marine Microbiology, 28195, Germany
[4]MARUM, University of Bremen, Bremen, 28195, Germany

10 *Correspondence to*: C. Chad Lloyd (cclloyd@unc.edu)

Abstract. Heterotrophic bacteria process nearly half of the organic matter produced by phytoplankton in the surface ocean. Much of this organic matter consists of high molecular weight (HMW) biopolymers such as polysaccharides and proteins, which must initially be hydrolyzed to smaller sizes by structurally specific extracellular enzymes. To assess the relationships between substrate structure and microbial community composition and function, we concurrently determined carbohydrate

15 abundance and structural complexity, bacterial community composition, and peptidase and polysaccharide hydrolase activities throughout the water column at four distinct stations in the western North Atlantic Ocean. Although the monosaccharide constituents of particulate organic matter (POM) were similar among stations, the structural complexity of POM-derived polysaccharides varied by depth and station, as demonstrated by polysaccharide-specific antibody probing. Bacterial community composition and polysaccharide hydrolase activities also varied by depth and station, suggesting that the structure

20 and function of bacterial communities—and the structural complexity of their target substrates—are interlinked. Thus, the extent to which bacteria can transform organic matter in the ocean is dependent on both the structural complexity of the organic matter and their enzymatic capabilities in different depths and regions of the ocean.

Short Summary. The cycling of carbon throughout the ocean is dependent on the balance between phytoplankton productivity

25 and heterotrophic decomposition. Bacteria must produce structurally specific enzymes to degrade specific chemical structures found in organic matter. We found distinct correlations between the organic matter composition, bacterial community structure, and potential enzymatic activities with depth, and found that the structural complexity of organic matter varies with location in the ocean.

1 Introduction

30   Carbohydrates and proteins are the major macromolecular components of the phytoplankton-derived organic matter (Wakeham et al., 1997; Hedges et al., 2002) that forms the base of marine food webs. Much of this organic matter is processed

by heterotrophic bacterial communities (Azam and Malfatti, 2007), which use extracellular enzymes to hydrolyze high molecular weight (HMW) organic matter to sizes suitable for uptake. These extracellular enzymes have high structural specificity (Lombard et al., 2014). Thus, within a community, some member(s) must produce the requisite enzymes to

35 hydrolyze a substrate in order for it to be consumed. Recent work has demonstrated that the genes encoding diverse types of enzymes differ among distinct bacteria (Avci et al., 2020, Krüger et al., 2019). In addition, our previous investigations have shown that the enzymatic activities of microbial communities vary with depth and location in the ocean (Arnosti et al., 2011; Steen et al., 2012; Hoarfrost and Arnosti, 2017; Balmonte et al., 2021). However, the cues to which these microbial communities are responding—in particular, the structure of the macromolecules that they sense and target—have to date not

40 been well characterized. This long-standing knowledge gap (Hedges et al., 2001) is due in part to the difficulties of characterizing intact macromolecules. Due to the multitude of possible linkages between individual monomers (Laine, 1994; Arnosti et al., 2021), little progress has been made on characterization of polysaccharides, despite advances in 'omics technologies, such as proteomics, which have enabled identification of protein structures (Morris et al., 2010; Saito et al., 2019; Francis et al., 2021). In the past decade, advances in biotechnology have made possible the detection of intact polysaccharides

45 in marine environments (Vidal-Melgosa et al., 2021; Buck-Wiese et al., 2023), but to the best of our knowledge, to date these approaches have been used only once in the open ocean (Priest et al., 2023).

The structure of a high molecular weight substrate is therefore difficult to determine. Nonetheless, it is an important consideration, since structural features likely determine the types of enzymes needed to degrade it. For polysaccharides, the number of distinct linkages scales linearly with the number of enzymes required for hydrolysis (Bligh et al., 2022); the number

50 to hydrolyze proteins may be smaller, since peptidases likely have a broader substrate specificity (Lapébie et al., 2019). The enzymatic capabilities of heterotrophic bacterial communities thus help determine which organic matter is labile and therefore easily consumed, and what fraction is recalcitrant for a given community (Arnosti, 2011; Arnosti et al. 2021). For example, a simple polysaccharide such as laminarin may only require three enzymes to degrade (Becker et al., 2017), whereas a comparatively complex polysaccharide, such as fucoidan, can require hundreds of enzymes to fully degrade (Sichert et al.,

55 2020).

To investigate the interrelationships among extracellular enzymes, the complex substrates they target, and microbial communities, we measured the activities of enzymes targeting polysaccharides and proteins through the water column at four distinct sites in the western North Atlantic that are characterized by different water masses and productivity regimes. At each station we measured the activities of polysaccharide- and peptide-hydrolyzing enzymes, collected particulate organic carbon

60 (POC), and determined the monosaccharide constituents of combined carbohydrates from POC as well as the structural complexity of polysaccharides extracted from the POC. We simultaneously collected samples to determine bacterial community composition. Although previous investigations have compared bacterial community composition with polysaccharide hydrolase activities (e.g., Murray et al., 2007; Teske et al., 2011; Arnosti et al., 2012; Balmonte et al., 2018; Giljan et al., 2023; Lloyd et al., 2023), this is the first study to investigate the structure and abundance of the combined

65 carbohydrates the communities may target. Moreover, this is one of very few studies (Priest et al., 2023) that uses new

analytical approaches to quantify carbohydrate inventories in the open ocean, and is the first to compare them to polysaccharide hydrolase activities. This study thus offers insights into the functional capabilities of bacteria throughout the water column, as well as of the substrates that they target.

2 Methods

2.1 Stations and water sampling

Water samples were collected in the western North Atlantic aboard R/V *Endeavor* (cruise EN638; May 15th—May 30th, 2019). Samples were collected at one shelf station and three open ocean stations (Stns. 17 and 18-20, respectively; Fig. 1) using a Niskin rosette (12 x 30L bottles) equipped with a Seabird 32 CTD. Data for T, S, O₂, and chlorophyll concentrations (Table 1) are all from the Seabird CTD sensors. At each offshore station, water was collected from the surface, deep chlorophyll maximum (DCM), 300 m, the lower mesopelagic (typically between 600 and 850m), 1500 m, 3000 m, and bottom (ranging from 3190 – 5580 m). At Stn. 17, water was collected from the surface, DCM, and bottom (depth: 625 m). Seawater was transferred from Niskin bottles into 20 L carboys that were acid washed and rinsed with RO (reverse osmosis) water, then rinsed three times with seawater from the sampling depth prior to filling. Transfers were carried out using silicone tubing that had been acid washed and rinsed with distilled water prior to use. Seawater was taken directly from the carboys to measure bacterial protein production, polysaccharide hydrolase activities, peptidase activities, and glucosidase activities, as described below.

2.2 Bacterial production and cell counts

2.2.1 Bacterial productivity

Bacterial productivity was measured after Kirchman et al. (2001), using incorporation of tritiated leucine (^{3}H-Leu; 20 nM). In brief, leucine incorporation rates were measured in samples incubated in the dark at *in-situ* temperatures, and were converted to bacterial carbon production through multiplication by a factor of 0.86 (Simon and Azam, 1989; Kirchman, 2001).

2.2.2 Bacterial cell counts

Seawater samples were fixed with formaldehyde at a final concentration of 1%, then 25-50 mL of the fixed samples were filtered through a polycarbonate filter (pore size: 0.22 µm) at a maximum vacuum of 200 mbar. DNA staining was done using 4′,6-Diamidin-2-phenylindol (DAPI), and samples were mounted with a Citifluor/VectaShield (4:1) solution.

Cell counting was done using a fully automated epifluorescence microscope (Zeiss AxioImager.Z2 microscope stand, Carl Zeiss) and image analysis was carried out as described by Bennke et al. (2016). Cell count verification of the automated image analysis was done manually.

2.3 Organic matter analyses

95 **2.3.1 Collection of particulate organic matter**

Particulate organic matter (POM) was collected by filtering between 5-15 liters of water through a 47-mm pre-combusted glass fiber filter (GF/F; nominal pore size 0.7 um; Table S1). These samples were collected at all depths and stations.

2.3.2 Particulate organic carbon and particulate organic nitrogen

100 Particulate organic carbon (POC) and particulate organic nitrogen (PON) were measured as described in Becker et al (2020). In brief, triplicate filter punches from samples collected on pre-combusted glass fiber filters (GF/F) were placed in an acidic environment (concentrated HCl fumes) for 24 h to remove inorganic carbon. After drying for 24 h at 60 °C, the samples were packed in pre-combusted tin foil. C and N were quantified using an elemental analyzer (cario MICRO cube; Elementar Analysensysteme) using sulfanilamide for calibration.

105 **2.3.3 Monosaccharide composition of POM**

POM samples were collected as described above. The monosaccharide constituents of the total combined carbohydrates (i.e., polysaccharides, glycoproteins, glycolipids, etc.) were determined from triplicate filter punches (11.2 mm diameter). Samples were acid hydrolyzed by adding 1 M HCl to each filter piece, flame sealing each piece in a glass ampule, and placing the ampules in a drying oven at 100°C for 24 hours. After acid hydrolysis, the samples were dried on a speed-vac 110 and resuspended in Milli-Q to remove any HCl. The quantity and composition of the resulting monosaccharides were measured using a modified protocol (Engel and Handel (2011), as described by Vidal-Melgosa et al. (2021)). In brief, neutral, amino, and acidic sugars were quantified using high performance anion exchange chromatography on a Dionex ICS-5000+ system with pulsed amperometric detection (HPAEC-PAD). Peaks were identified using retention times of purified monosaccharide standards; abundance was quantified from standards using the peak area for a given monosaccharide.

115 **2.3.4 Polysaccharide extraction for microarray analyses**

POM samples were prepared for polysaccharide analysis according to Vidal-Melgosa et al. (2021). Polysaccharides were sequentially extracted from four filter piece punches (11.2 mm diameter) from the GF/F filter. The samples were first extracted with autoclaved MilliQ water, followed by 50 mM EDTA, and finally 4 M NaOH with 0.1% NaBH$_4$. The supernatant containing extracted polysaccharides was collected from each of the sequential steps and stored at 4 °C.

120 **2.3.5 Carbohydrate microarray analysis**

The polysaccharides extracted as described above were analyzed following Vidal-Melgosa et al. (2021). In brief, the polysaccharide extracts were first diluted in printing buffer (55.2% glycerol, 44% water, 0.8% Triton X-100), and then printed

on 0.45 µm pore size nitrocellulose membrane (Whatman) using a microarray robot (Sprint, Arrayjet, Roslin, UK) at 20 °C and 50% humidity. The membranes were probed with one of 9 monoclonal antibodies, washed multiple times, and probed
125 with secondary antibodies (anti-rat, anti-mouse, or anti-His tag) conjugated to alkaline phosphatase for 2 hours. The arrays were developed using 5-bromo-4-chloro-3-indolyphosphate and nitro blue tetrazolium in alkaline phosphatase buffer (100 mM NaCl, 5 mM $MgCl_2$, 100 mM Tris-HCl, pH 9.5). The microarrays were scanned and signal intensity was acquired using the software Array-Pro Analyzer 6.3 (Media Cybernetics). Signals were normalized amongst samples; higher signals correspond to a higher abundance of a given polysaccharide epitope.

130 **2.4 Analysis of bacterial community composition**

Bacterial community composition at all stations and sampling depth was assessed through 16S rRNA analysis. Seawater (25 mL) was filtered through a 0.22 µm pore size polycarbonate filter at a maximum vacuum of 200 mbar. The filters were air dried and frozen at -20 °C until further processing. Total DNA was extracted from these filters using the DNeasy Power Water Kit (Quiagen). The variable V3 and V4 regions (490 bp) of the 16S rRNA were amplified in 30 PCR cycles,
135 using the 5 PRIME HotMasterMix (Quantabio) together with the Bakt_314F (5' CCTACGGGNGGCWGCAG 3') and Bakt_805R (5' GACTACGVGGGTATCTAATCC 3') PCR primer pair (Herlemann et al., 2011). Forward and reverse primers were barcoded with individual 8 bp barcode adapter (based on the NEB Multiplex Oligos for Illumina, New England Biolabs). Each amplified PCR product was purified and size selected using the AMPure XP PCR Cleanup system (Beckman Coulter) before barcoded products were pooled in equimolar concentrations. The pools were sent to the Max Planck-Genome-Centre
140 (Cologne) for paired-end Illumina sequencing (2x250 bp HiSeq2500). Merging, demultiplexing and quality trimming (sequence length 300–500 bp, < 2% homopolymers, < 2 % ambiguities) of bulk sequences was done using BBTools (Bushnell, B., 2014). Sequence comparison and taxonomic assignment of the retrieved sequences was done using the SILVAngs pipeline (Quast et al., 2013) with the SSU rRNA SILVA database 138.

2.5 Enzymatic activity measurements

145 **2.5.1 Measurement of peptidase and glucosidase activities**

Alpha- and beta-glucosidase activities, the activities of enzymes that hydrolyze terminal glucose units from larger structures, were measured using small substrate proxies consisting of α-glucose and β-glucose linked to 4-methylumbelliferone (MUF). Exo-acting (terminal-unit cleaving) peptidase activities were measured using the amino acid leucine linked to the fluorophore 7-amido-4-methyl coumarin (MCA), whereas activities of endo-acting (midchain-cleaving) peptidases were
150 measured using short peptides linked to MCA. Chymotrypsin activities were measured with alanine-alanine-phenylalanine (AAF; 1-letter amino acid codes) and alanine-alanine-proline-phenylalanine (AAPF), and trypsin activities were measured with glutamine-alanine-arginine (QAR) and phenylalanine-serine-arginine (FSR).

Enzymatic activities were measured in seawater as previously described (Hoarfrost and Arnosti, 2017). In brief, substrate was added at saturating concentrations (150 µM as determined in surface seawater at Stn. 17) to a total volume of
155 200 µL in a 96-well plate. Samples consisted of triplicate wells of seawater amended with substrate for live incubations, and triplicate wells of autoclaved seawater amended with substrate were used for killed controls. Fluorescence was measured immediately (t0) and every 6 hours over 24 hours, using a plate reader (TECAN SpectraFluor Plus with 340 nm excitation, 460 nm emission). Fluorescence signals were converted to concentrations using standard curves of MUF and MCA fluorophores. Hydrolysis rates were measured as an increase in fluorescence over time. Activities reported here were averaged
160 using data collected during the first twelve hours of incubations.

2.5.2 Measurement of polysaccharide hydrolase activities

The activities of enzymes hydrolyzing distinct polysaccharides were measured using six fluorescently-labeled polysaccharides: pullulan, laminarin, xylan, fucoidan, arabinogalactan, and chondroitin sulfate (Arnosti, 2003). The polysaccharides (Sigma) were labelled with fluoresceinamine (Sigma) and characterized following Arnosti (2003).
165 For each substrate, three 15 mL centrifuge tubes were filled with unfiltered seawater for the live incubations and one 15 mL centrifuge tube was filled with autoclaved seawater to serve as a killed control. A single substrate was added to each tube to a final concentration of 3.5 µM (except fucoidan which was added to a final concentration of 5 µM). One 15 mL centrifuge tube with autoclaved seawater served as a negative control, and one 15 mL centrifuge tube filled with bulk seawater served as a blank. Incubations were stored in the dark at close to *in situ* temperatures. For surface, DCM, 300 m, and bottom
170 water depths, larger incubations (600 mL) were set up (at the same final concentrations as above) to enable additional volume for analyses reported elsewhere (Giljan et al., 2023).

Subsamples were taken directly after each incubation was set up (day 0) and at five additional timepoints (3 days, 5 days, 10 days, 15 days, and 30 days) to measure hydrolysis rates. At each timepoint, 2 mL of water was collected from each sample and filtered (0.2 µm SFCA filter) into an epi tube, stored frozen at -20 C until analysis.
175 Hydrolysis of the six polysaccharides was measured using gel permeation chromatography with fluorescence detection (Arnosti 2003). The samples were injected onto a series of columns (a G50 Sephadex gel column followed by a G75 Sephadex gel column), and fluorescence was measured using a Hitachi detector set to excitation and emission wavelengths of 490 nm and 530 nm, respectively. Polysaccharide hydrolase activities were calculated by measuring the change in the relative proportion of signal in different molecular weight bins over time. Polysaccharide hydrolysis rates measured in surface waters,
180 and at the DCM, 300 m, and bottom waters were previously reported in Giljan et al. (2023).

2.6 Statistical analyses

2.6.1 NMDS plots

Non-metric multidimensional scaling (NMDS) plots using the Bray-Curtis dissimilarity index were constructed to visualize dissimilarities in peptidase and glucosidase activities, polysaccharide hydrolase activities, and bacterial community composition. Analysis of variance (ANOVA) was used to test differences in enzymatic activity and carbohydrate content between stations and depths.

2.6.2 Correlation plots

To visualize correlations between collected environmental data and enzyme activities, correlation plots were constructed using Corrplot (v. 0.92) in R (v. 4.2.1 Patched). Since environmental parameters varied considerably by station (Table 2), correlation plots were also constructed for each station. In addition, a Corrplot was constructed by depth, with the surface and DCM classified as epipelagic; 300 m, 800/850 m, and 1500 m as mesopelagic; and depths below 1500 m as bathypelagic.

3 Results

### 3.1 Distinct water mass characteristics at each station

Stations differed considerably in the physical and chemical characteristics of the water masses, especially in surface waters (Fig. 1; Table 2). At Stn. 17, located on the continental slope (maximum depth: 625 m), surface water and DCM water both were characteristic of Gulf Stream Water (Liu and Tanhua, 2021). Bottom water collected at Stn. 18 was characteristic of upper Labrador Sea Water (Heidrich and Todd, 2020; Andres et al., 2018). Surface water at Stn. 18 also had characteristics of Gulf Stream water. This water was warmer and more saline (25.18°C and 36.42 PSU) than surface waters at Stns. 19 (8.78°C and 33.72 PSU).

Surface water from Stn. 19, near the continental shelf break off Newfoundland, had characteristics similar to the Labrador Current that flows south past the Grand Banks (Fratantoni & Pickart, 2007). The salinity at this station increased by 1 PSU between surface/DCM waters and a depth of 300 m, resulting in the strongest measured vertical gradient of salinity with depth (Fig. 1). The relatively fresh surface water at Stn. 19 likely indicates the influence of sea ice melt, or potentially also freshwater drainage from the Gulf of St. Lawrence (Fratantoni and Pickart, 2007). The physicochemical characteristics of water samples collected at the surface, DCM, and 300 m at Stn. 19 were similar in density and salinity to those of the Warm Slope Water and Labrador Slope Water measured by Fratantoni & Pickart (2007). The water at 300 m at Stn. 19 also corresponded to an oxygen minimum, with an O_2 concentration of 135 µmol kg^{-1}, as measured by the CTD sensor.

Stn. 20 was located within the North Atlantic subtropical gyre. Stn. 20 surface water was characteristic of Thermocline Water (Heidrich and Todd, 2020). The T/S characteristics of water collected at depths of 300 m were very similar at Stn. 20

and Stn. 18, and was likely Eighteen Degree Water (Heidrich and Todd, 2020). Stn. 20 water collected at 1500 m, 3000 m, and just above the seafloor had similar characteristics at Stns. 18-20, and the T/S characteristics were most similar to North Atlantic Deep Water (Fig. 1; Broecker, 1991). Stns. 17 and 18 were located within the Gulf Stream, while Stn. 20 was located within the oligotrophic Sargasso Sea (Fig. 1; Liu and Tanhua, 2021).
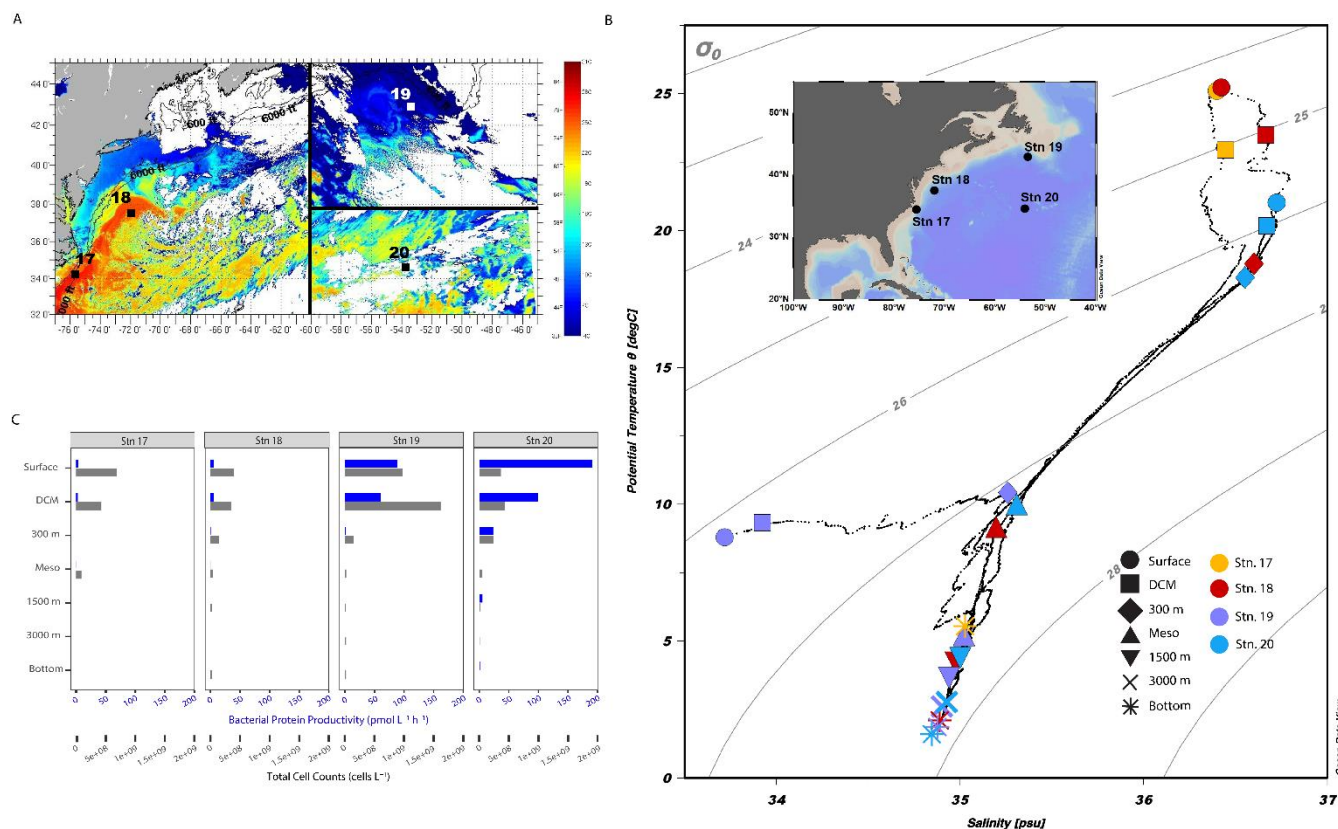
215

Figure 1: Physical and chemical characteristics of sampling stations within the western North Atlantic. (A) Sea surface temperature, acquired by satellite imaging (Rutgers University), on/around the sampling day at each station. (B) Temperature and salinity diagram of the four stations highlights the differences in water masses sampled. Shapes denote the depths; colors denote the stations. (C) Bacterial cell counts (black) and protein productivity (blue) of each sampling station/depth. Note the differences between the axes for bacterial cell counts and bacterial productivity.

220

3.2 POC concentrations

Overall, POC concentrations were highest in surface and DCM waters, and decreased with depth (Suppl. Fig. 1). The highest POC concentrations in surface and DCM waters were measured at Stn. 19, the same depths with high chlorophyll fluorescence and high particulate organic nitrogen (PON) values (Table 2). In the offshore stations, POC concentrations

225 increased slightly at bottom depths compared to the depths measured above. Overall, PON values also decreased with depth.

3.3 Monosaccharide composition of POM-derived combined carbohydrates

The monosaccharide constituents of POM-derived combined carbohydrates were very similar in surface and DCM waters of all stations (ANOVA, $p = 0.90$), but changed markedly with depth (Fig. 2). In subsurface waters, these constituents were significantly different from the constituents in surface and DCM waters (ANOVA, $p = 0.026$). In surface waters at all

230 stations, glucose, xylose, and galactose composed ~80% or more of the total combined carbohydrates. Although fucose, galactosamine, arabinose, glucosamine, and glucuronic acid composed ~20% or less of total combined carbohydrates, they were more abundant in surface waters and decreased considerably in relative abundance with depth (Fig. 2). Galactosamine and arabinose were only detected in surface and DCM waters offshore, and at all depths at Stn. 17. Overall, the concentration of POM-derived combined carbohydrates in seawater decreased with depth as well, ranging from 6-28 µg/L in surface waters

235 to ~0.5-1 µg/L in bottom waters, as expected (Fig. 2).

In the upper water column, total concentrations of monosaccharides contributing to combined carbohydrates differed somewhat by station (Fig. 2b; ANOVA, $p = 0.014$). Stn. 19 had the highest concentration (~28 µg L^{-1} in surface waters), consistent with the high chlorophyll fluorescence and high POC concentration at this station. At Stns. 18 and 20, the concentrations were much lower (~6 µg L^{-1}). Stn. 17 (with a total water column depth of ca. 600 m) also had higher total

240 concentrations in both surface and bottom waters, as well as somewhat different monosaccharide constituents than at the other stations (Fig. 2). At Stns. 18-20, there were no station-specific differences in monosaccharide composition in waters below DCM (ANOVA, $p = 0.58$).
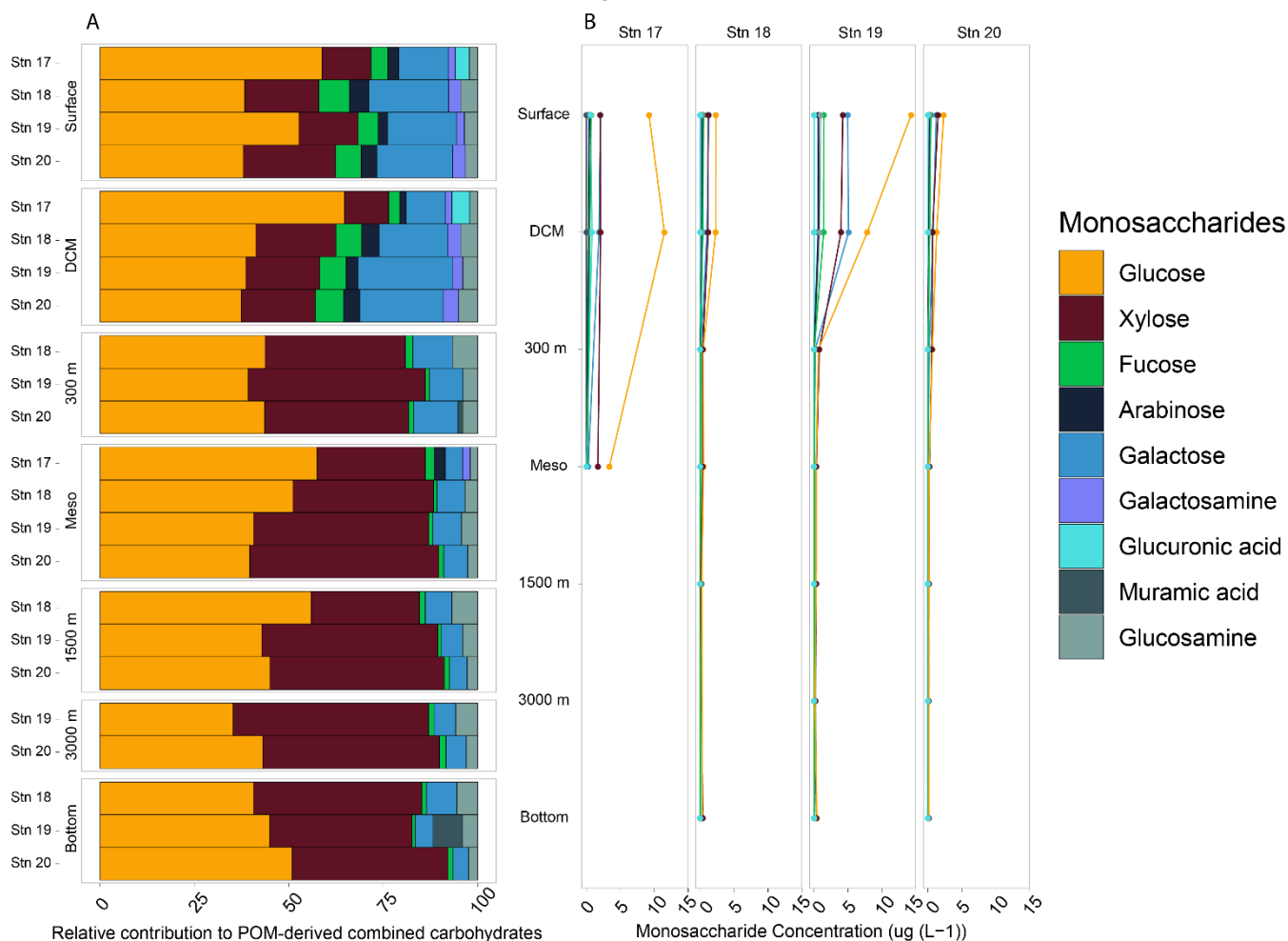
Figure 2: Monosaccharide constituents of the combined carbohydrates. (A) The relative contribution of the combined carbohydrates shows what percentage of the polysaccharides each monosaccharide represents. (B) The concentration of each monosaccharide, as determined by HPAEC-PAD.

3.4 Polysaccharide structures detected via microarray analysis

The carbohydrate epitopes—and therefore the structural complexity of polysaccharides—differed among stations (Fig. 3; ANOVA, p = 0.014). Polysaccharide structures extracted from POM were typically only detected in surface and DCM waters (except for the β-1,4-mannan detected in the comparatively shallow bottom water at Stn. 17 (Fig. 3)). At Stn. 17, microarray analysis identified fucoidan, β-1,3-glucan, and alginate in surface waters, while only β-1,3-glucan and alginate were identified at the DCM (Fig 3). β-1,4-mannan was detected in bottom waters (at 625 m), but not at any other depths for this station. For Stns. 18-20, specific polysaccharides were only detected in surface and DCM waters, where β-1,3-glucan and alginate were identified at all three stations. Fucoidan was detected in both surface and DCM waters at Stn. 19, but only in

255 surface waters at Stn. 20. Both epitopes of fucoidan were detected in Stn. 20 surface waters, and fucoidan had the highest

relative signal of any polysaccharides measured at any station and depth. Rhamnogalacturonan I (RGI), β-1,4-mannan, and

xylol residues were additionally identified in Stn. 19 surface and DCM waters.
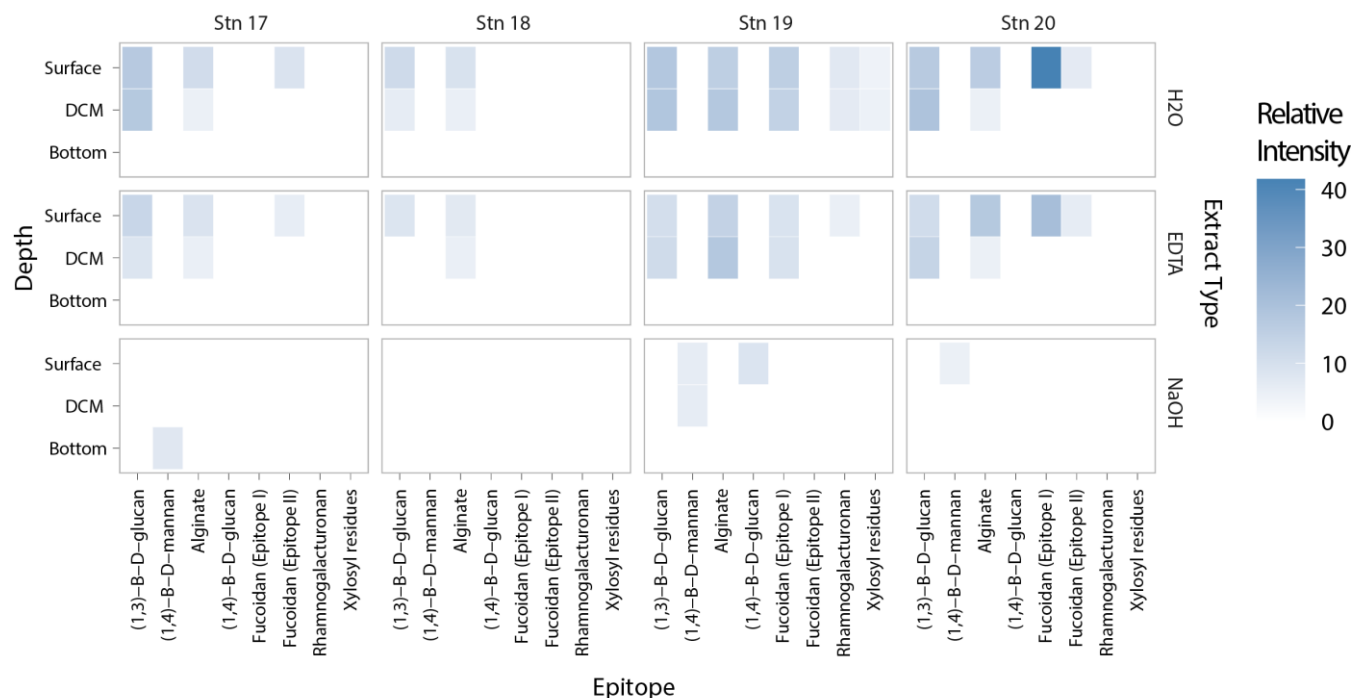
Figure 3: Heatmap of detected polysaccharides from the carbohydrate microarrays. Darker shades represent a higher relative
260 **intensity. Note: the carbohydrate microarrays are only semiquantitative; while comparisons can be made between the individual**
stations and depths of a given epitope, they cannot be used to compare between different epitopes. Depths between DCM and bottom
waters were removed, as no epitopes were detected in any of those samples.

3.5 Total cell counts and bacterial protein productivity

At all stations, total microbial cell counts were highest in the upper water column and decreased with depth. At Stn.
265 19, surface and DCM waters had much higher total cell counts than those at the same depths at Stns. 17, 18, and 20; these high

total cell counts coincided with the greater chlorophyll-α levels at Stn. 19 (Fig. 1; Table 2). Cell counts ranged from $0.3 – 1.0$

$x10^9$ cells L^{-1} in surface waters, to ca. $1.0 – 2.0$ $x10^8$ cells L^{-1} at 300 m, to as few as $0.8 – 1.3$ $x10^7$ cells L^{-1} in bottom water at

Stns. 18 – 20 (Fig. 1; Table 2). Cell counts were highest by far in the upper water column at Stn. 19, where total cell counts at

the DCM (1.62 x 10^6 cells mL^{-1}) were almost twice as high as in surface waters (9.71 x 10^5 cells mL^{-1}; Table 1). At Stn. 20,
270 cell counts at the DCM were somewhat higher than in surface waters, but the difference between depths was smaller.

Cell-specific bacterial productivity increased in surface waters from the inshore Stn. 17 at 6 $x10^{-9}$ pmol $cell^{-1}$ L^{-1} by

two orders of magnitude to 5 $x10^{-7}$ pmol $cell^{-1}$ L^{-1} at the offshore, open-ocean Stn. 20 (Fig. 1; Suppl. Fig. 2). At Stn. 17,
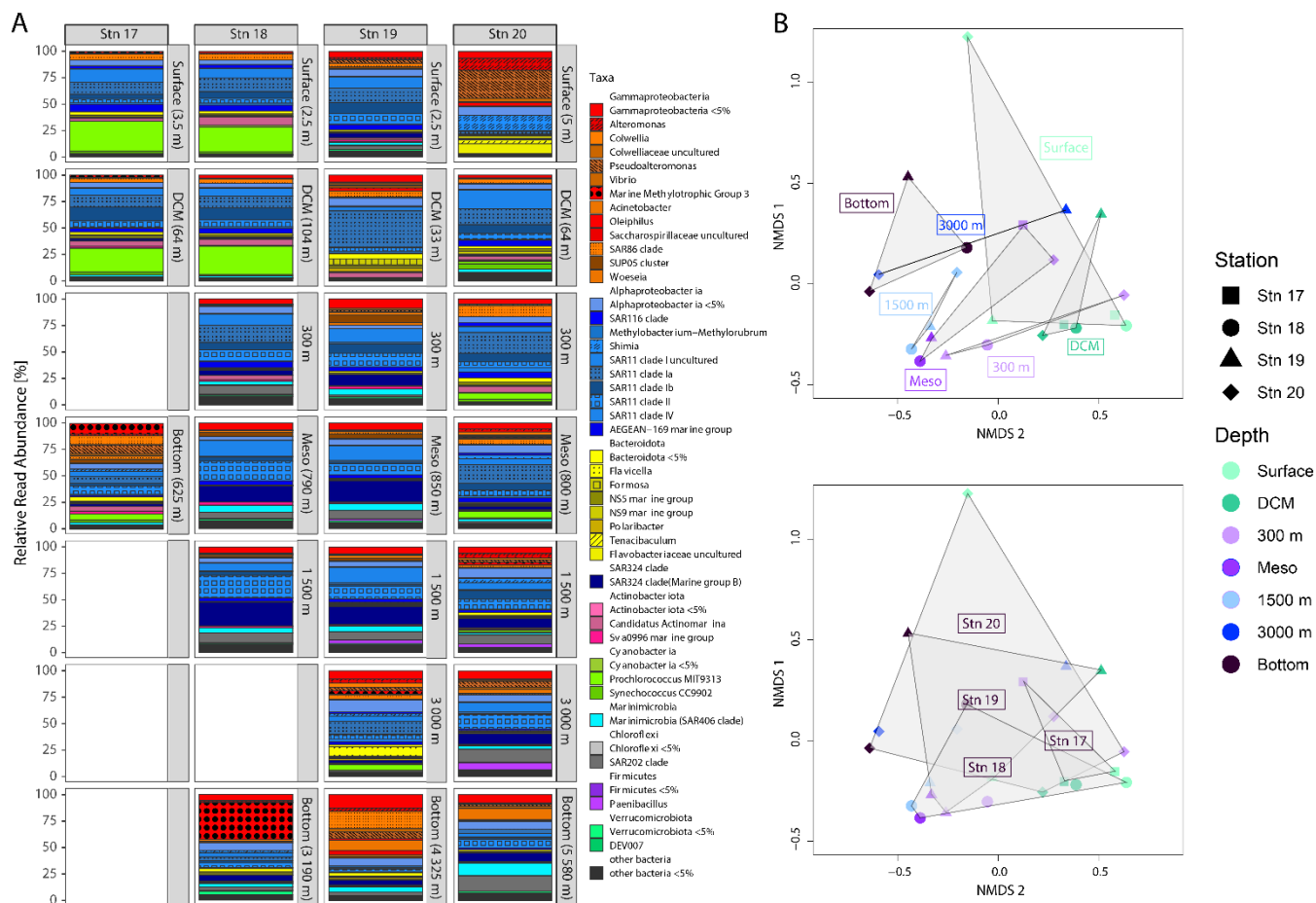
productivity increased slightly at the DCM compared to the surface, but was undetectable in bottom waters. At Stns. 18 – 20, bacterial productivity decreased considerably within the first 300 m of the water column, followed by a productivity peak at

275   the lower mesopelagic at Stn. 18 and at 1500 m at Stns. 19 and 20, respectively. While protein productivity roughly doubled at this depth at Stns. 18 and 19, the productivity increased 26-fold to 2×10^{-7} pmol cell^{-1} L^{-1} at Stn. 20. These peaks are followed by a decrease in bacterial productivity with depth, and a slight increase again in bottom waters. The total bacterial productivity in bottom waters increased the further offshore the stations were (Fig. 1).

3.6 Community composition

280   The bacterial communities in surface and DCM waters at all four stations were mainly composed of members of the Proteobacteria (Gamma- and Alphaproteobacteria), the Bacteroidetes, Actinobacteria, and Cyanobacteria. In waters at 300 m and below, higher relative abundances of the SAR324 clade, Marinimicrobia, Chloroflexi and Firmicutes were detected (Fig. 4), Bacteroidetes and Actinobacteria were present in lower relative numbers, and Cyanobacteria had virtually disappeared.

          Bacterial community composition in surface and DCM waters differed among stations, and – for Stns. 19 and 20 –
285   by depth. At Stns. 17 and 18, the surface water and the DCM communities were quite similar, with a large contribution (~30%) of Prochlorococcus (Fig. 4a, b), but these communities differed considerably from the other stations. Surface waters of Stn. 19 were dominated by Alphaproteobacteria, which constituted ~50% of the total community. These waters also included Chloroflexi, Marinimicrobia and members of the SAR324 clade, which were not detected in other surface water communities. Bacterial community composition of DCM waters at Stn. 19 was quite different (Fig. 4), however, with one clade of the SAR11
290   dominating. In addition, Bacteroidetes were present in greater abundance and showed greater diversity than at other sampling locations. In Stn. 20 surface waters, Gammaproteobacteria, mainly *Colwellia* and *Alteromonas,* were present in high abundance. They accounted, together with uncultured Flavobacteriaceae and the alphaproteobacterial *Shimia,* for most of the community. Stn. 20 DCM waters were dominated by Alphaproteobacteria, and were distinguished from surface waters particularly by the presence of Synechococcus.

Figure 4: (A) Relative abundance of bacterial community composition. Operational taxonomic units are grouped by similar colors; select taxa are differentiated by pattern for better visualization. Non-metric multidimensional scaling (NMDS) plot based on Bray-Curtis dissimilarity shows bacterial communities clustered by (B) depth and (C) station.

Bacterial communities in subsurface waters at each station differed substantially from their surface counterparts. Stn. 17 bottom water (at 625 m) had a strong representation of Gammaproteobacteria (~35% of the community), while the contribution of Prochlorococcus and Alphaproteobacteria decreased relative to the surface and DCM. At Stn. 18, the communities at 300 m, the lower mesopelagic, and 1500 m were relatively similar, and showed similarity to communities at those same depths at Stn. 19 (Fig. 4). These communities were dominated by Alphaproteobacteria, with contributions from members of Marinimicrobia, SAR324, and SAR202. For Stn. 18, the Gammaproteobacterial contribution at this depth was the lowest observed at all stations and depths. Stn. 20 subsurface communities differed slightly among depths, and were distinct from the subsurface communities of Stns. 18 and 19. Notably, at Stn. 20, Prochlorococcus was also detected at depths of 300 m, as well as in the lower mesopelagic, and at 1500 m. Stn. 20 communities were also dominated by Alphaproteobacteria, with minor contributions from Bacteroidetes at 300 m and 1500 m.
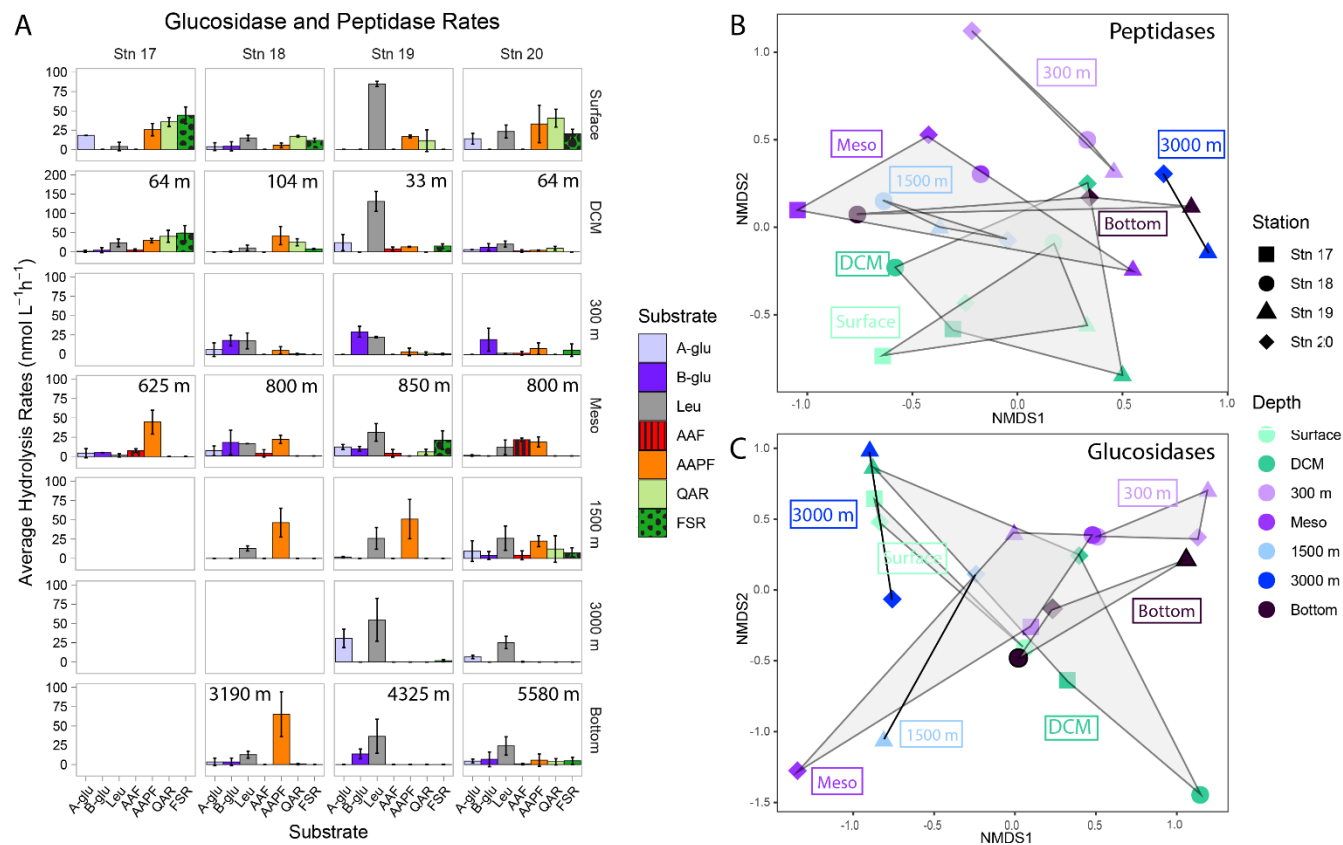
13

In the deepest waters, at more than 3000 m depth, the bacterial communities were quite different among stations. The
310 bottom water community at 3190 m at Stn. 18 stands out based on the dominant ~30% of *Alteromonas*, a unique presence of
the verrucomicrobial DEV007, and the presence of some Bacteroidetes. Bacteroidetes were also detected in 3000 m and bottom
waters at Stn. 19. This phylum was very reduced in relative abundance at Stns. 18 and 19 at depths between 300 to 1500 m,
but made up to 15% of the population at 3000 m. Also at Stn. 19, a wide array of members of Gammaproteobacteria accounted
for ~25% of the population at a depth of 3000 m. Gammaproteobacteria increased to more than 50% relative abundance in Stn.
315 19 bottom water, with a contribution of different taxa; this community was distinct from Stn. 18 bottom water, where the
Gammaproteobacteria were dominated by *Marine Methylotrophic Group 3*. In Stn. 20 bottom waters, the SAR324 clade,
Chloroflexi and Marinimicrobia increase in relative abundance, together accounting for up to 40 % of the community.
Firmicutes were present in comparatively high at abundance 3000 m, but absent in bottom water, where we detected a small
contribution of Verrucomicrobia. The relative abundance of Bacteroidetes in waters deeper than 3000 m at Stn. 20 was quite
320 small, contrasting with the high relative abundance of Bacteroidetes found in surface waters at this station.

In general, Stn. 20 showed the greatest distinctions with depth among bacterial communities, and Stn. 17 (which was
on the continental shelf), the least. Overall, the bacterial community composition of the four stations was more distinct by
depth than by location (Fig. 4b, c). The surface water bacterial communities were the most distinct among the different stations
(Fig. 4), however.

325 **3.7 Glucosidase and peptidase activities**

Station as well as depth separation was notable among the peptidase and glucosidase activities, with differences in
both the rates and spectrum of glucose and peptide substrates hydrolyzed (Fig. 5; Suppl. Fig. 3). At Stn. 19, leucine
aminopeptidase activity tended to dominate at all depths, whereas at Stns. 17, 18, and 20, endopeptidase activities were
frequently comparable to leucine aminopeptidase activities. Alpha- and beta-glucosidase activities were prominent particularly
330 at 300 m and ca. 800 m (Fig. 5).

In general, summed glucosidase and peptidase activities at 3000+ m depths were only slightly lower than at shallower
depths. Summed activities were highest at surface and DCM waters (upwards of 100 nmol L^{-1} hr^{-1}), then decreased by half (to
upwards of 50 nmol L^{-1} hr^{-1}) below 300 m (Suppl. Fig. 4). Fewer substrates were typically hydrolyzed at deeper depths,
although Stn. 20 showed hydrolysis of all seven glucosidase and peptidase substrates at 1500 m as well as in bottom water
335 (Fig. 5). At Stn. 18, one endopeptidase, chymotrypsin substrate AAPF, was hydrolyzed more rapidly at deeper depths (depths
at the lower mesopelagic and below), with particularly high activity in bottom water. In contrast, leucine aminopeptidase
activities were generally high at all depths at Stn. 19, and was the highest peptidase activity at depths of 1500m and below at
Stn. 20.

Figure 5: (A) Average glucosidase and peptidase activities for each station and depth; error bars represent the standard deviation of activities measured over 12 hours. Note that y-axes differ between each depth. A-glu = α-glucosidase; b-glu = β-glucosidase; leu = Leucine aminopeptidase; AAF = alanine-alanine-phenylalanine; AAPF = alanine-alanine-proline-phenylalanine; QAR = glutamine-alanine-arginine; FSR = phenylalanine-serine-arginine. Non-metric multidimensional scaling (NMDS) plot based on Bray-Curtis dissimilarity shows **(B)** peptidase and **(C)** glucosidase activities clustered by depth. Shapes represent stations; colors represent depths.

3.8 Polysaccharide hydrolase activities

Polysaccharide hydrolase activities varied primarily by depth (Fig. 6). The spectrum of enzyme activities (the number of different polysaccharides) was generally broadest not in surface waters, where three or fewer polysaccharide substrates were hydrolyzed, but the DCM, at 300 m, in the lower mesopelagic (ca 800 m), or at 1500 m depth, where generally four or five substrates were hydrolyzed (Fig. 6). Stn. 18 lower mesopelagic and Stns. 19 and 20 1500 m waters showed increased polysaccharide hydrolase activities compared with other stations at the comparable depths; these activities are also reflected in the bacterial productivity data (see above; Figs. 1,6). Summed polysaccharide hydrolase activities were lower in 3000+ m waters (~1-4 nmol monomer L^{-1} hr^{-1}) compared to surface, DCM, 300 m, and lower mesopelagic waters waters (~2-20 nmol monomer L^{-1} hr^{-1}; Suppl. Fig. 5). At deeper depths, enzymatic activities were also generally first detected at later timepoints compared to shallower depths (Fig. 6).
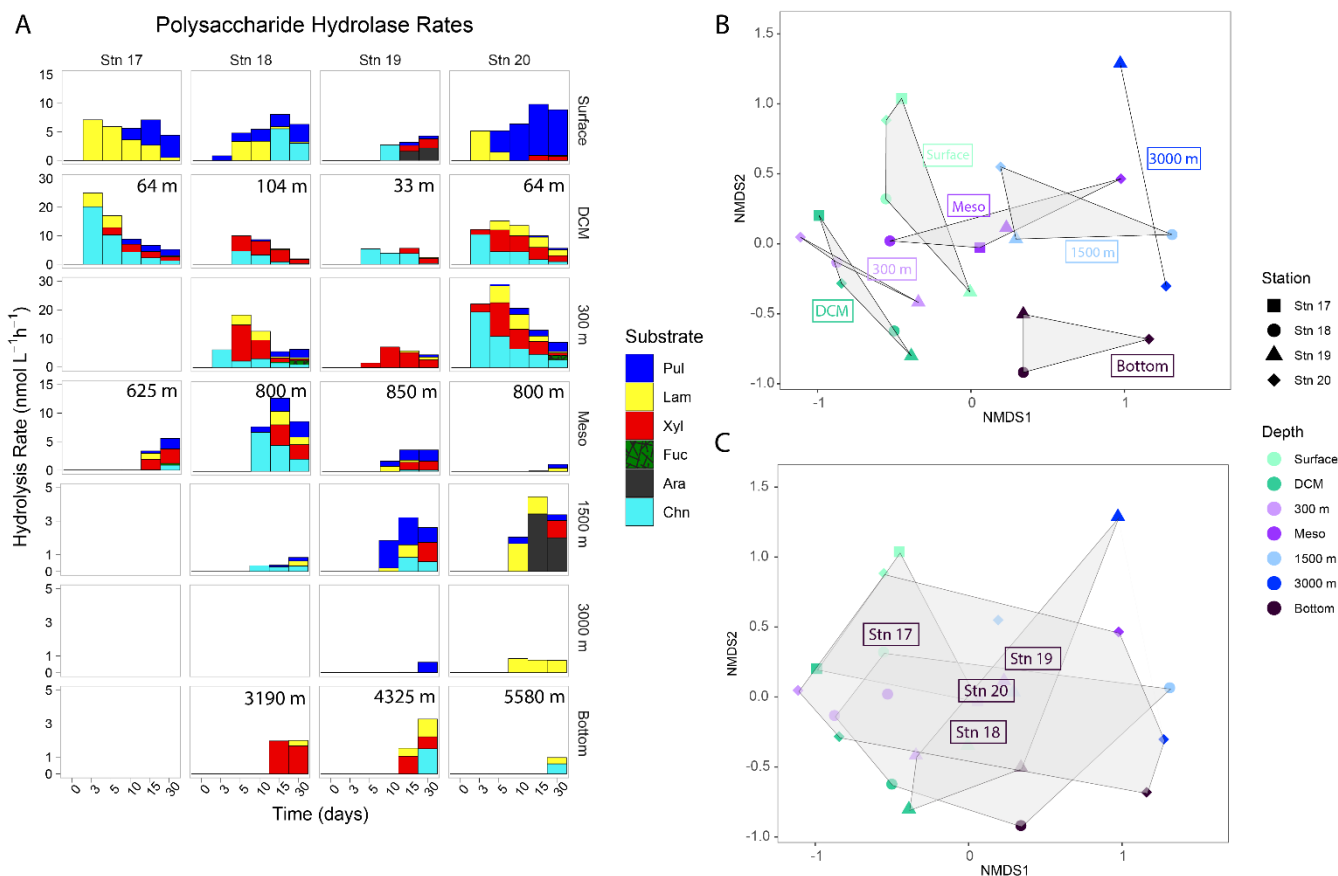
Figure 6: (A) Polysaccharide hydrolysis activities for each station and depth; the hydrolysis rates for each timepoint are displayed to show when each substrate was hydrolyzed. Note that y-axes differ between each depth. Pul = Pullulan; Lam = Laminarin; Xyl = Xylan; Fuc = Fucoidan; Ara = Arabinogalactan; Chn = Chondroitin Sulfate. Non-metric multidimensional scaling (NMDS) plot based on Bray-Curtis dissimilarity shows polysaccharide hydrolysis rates clustered by (B) depth and (C) station. Shapes represent stations; colors represent depths.

Hydrolysis of pullulan, laminarin, chondroitin, and xylan was measurable at most stations and depths. Laminarin hydrolysis was measured in 19 of 23 distinct depths across stations, pullulan hydrolysis was measured in 18 depths across stations, xylanase activity was measured in 16 depths across stations, and chondroitin sulfate was hydrolyzed at 15 depths across stations. Fucoidan and arabinogalactan hydrolysis was rarely detected; fucoidan was only measurably hydrolyzed at 300 m at Stns. 18 and 20, and arabinogalactan was only measurably hydrolyzed in Stn. 19 surface waters and, notably, at Stn. 20 at 1500 m. No stations or depths showed hydrolysis of all six polysaccharides. Hydrolysis patterns were distinct by depth (Fig. 6b), but there was no discernible trend in regard to closeness of clustering of different depths; NMDS plots showed that stations broadly overlapped in terms of polysaccharide hydrolase activities.

3.9 Correlations among environmental parameters, carbohydrates, and enzymatic activities

A corrplot based on Pearson correlations was constructed to investigate connections among enzymatic activities, environmental parameters, and carbohydrate composition across all stations (Fig. 7). Notably, there was high correlation between total cell counts (TCC) and particulate organic carbon, chlorophyll a, and carbohydrate content (i.e., the constituent

375   monosaccharides of POC), including all monosaccharides except muramic and glucuronic acids. The majority of the monosaccharides—again, with the exception of muramic acid and glucuronic acid—were also highly correlated with one another (Fig. 7), as were those same monosaccharides and the polysaccharide epitopes to detect fucoidan, β-1,3-glucan, β-1,4-mannan, xylosyl residues, and alginate. Correlations among enzyme activities were evident in only a few cases (laminarinase with pullulanase; xylanase and fucoidanase; to a lesser extent, chondroitin sulfate hydrolase with laminarinase, xylanase, and

380   fucoidanase). QAR and FSR were highly correlated, and were also correlated with laminarinase and pullulanase; β-glucosidase was correlated with xylanase.
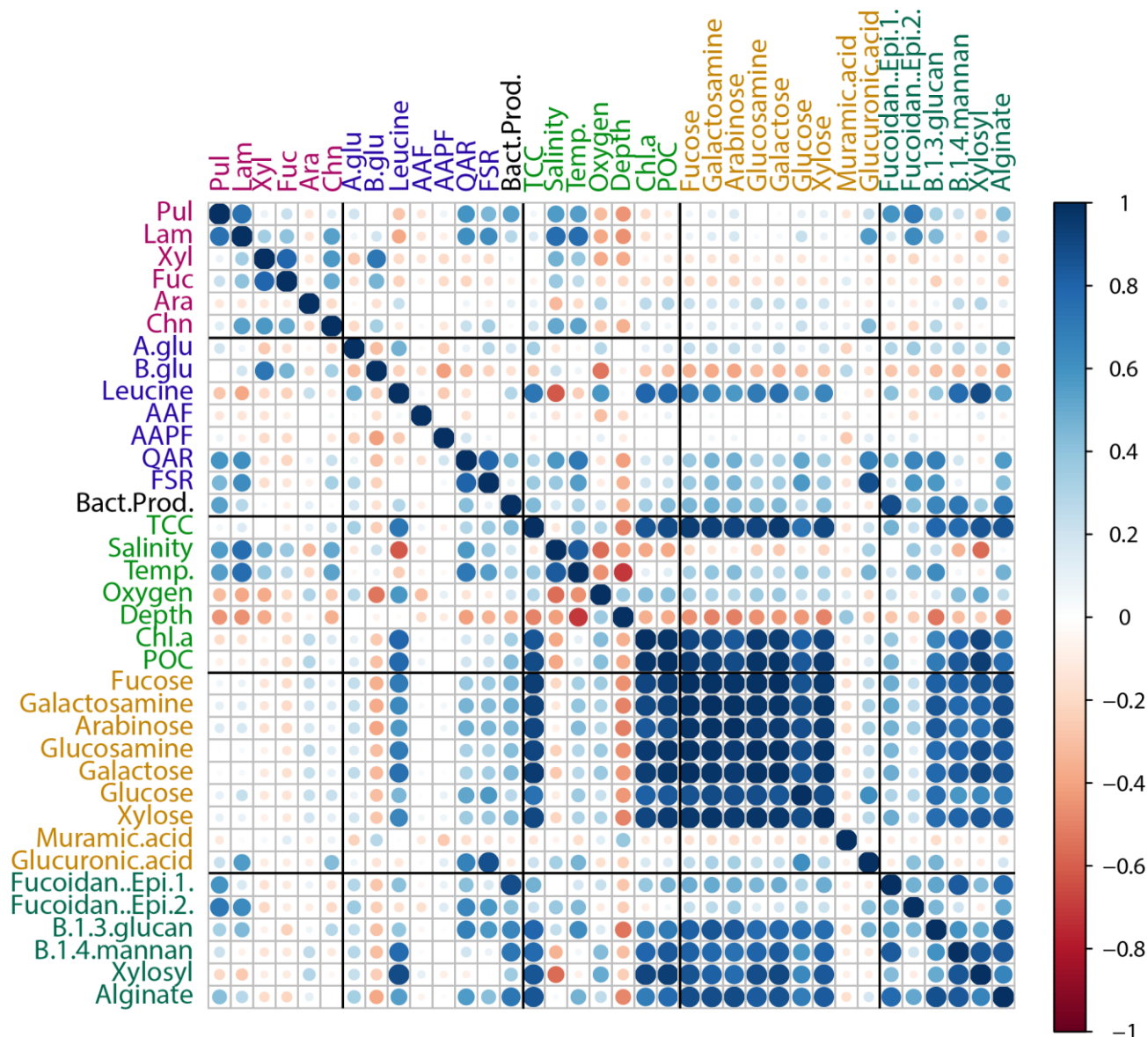
Figure 6: Correlation plot displaying Pearson's correlations between observed environmental parameters, carbohydrate inventories, and measured enzymatic activities for all samples. Blue denotes positive correlations while red denotes negative correlations. The shade and size of the circle emphasizes the intensity of correlation between environmental parameters, carbohydrate content, and enzymatic activities.

Given the physical and chemical distinctions among stations and depths (Table 2), we also constructed individual corrplots for each station (Suppl. Fig. 6). These plots differed considerably from one another and from the overall plot. For example, the polysaccharide hydrolases—aside from the correlations noted for the grouped stations (Fig. 7)—showed variable and distinctly different (i.e., positive/negative) correlations at individual stations as did α- and β-glucosidase and most of the peptidase activities (Fig. 7).

To view correlations among enzyme activities among stations for a given depth, three additional corrplots were constructed that grouped depths as either epipelagic (surface and DCM), mesopelagic (300 m, mesopelagic, 1500 m), or bathypelagic depths (3000 m and bottom water; Fig. 8). There are differences in correlations between polysaccharide hydrolase activities at each zone: in the epipelagic, there is a mix of positive and negative correlations, while in the bathypelagic, there are weaker positive correlations present (Fig. 8). The mesopelagic zone shows strong positive correlations between all of the polysaccharide hydrolase activities measured (Fig. 8). While the glucosidase and peptidase activities show a mix or correlations at each zone, there are strong positive correlations between QAR and FSR activity in all zones (Fig. 8).
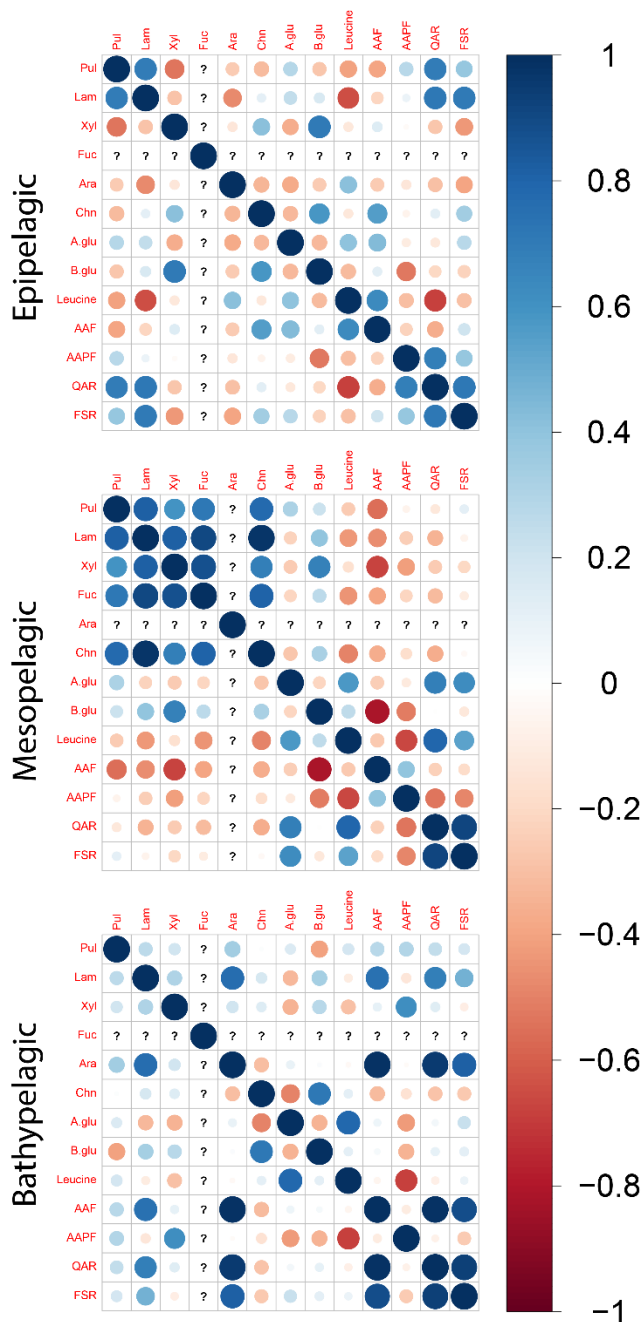
Figure 8: Correlation plots displaying Pearson's correlations between enzymatic activity measurements for at different depth zones. Epipelagic zone: surface and DCM waters; Mesopelagic zone: 300 m, 800/850 m, and 1500 m; Bathypelagic zone: >1500 m. Blue denotes positive correlations while red denotes negative correlations. The shade and size of the circle emphasizes the intensity of correlation between environmental parameters and enzymatic activities. (?) for a given column or row represents a lack of data required to assess a correlation for a given observation or measurement.

4 Discussion

The production and decomposition of marine organic matter is a function of interlinked oceanic processes and actors: marine productivity is powered by phytoplankton at the base of the food web by producing high molecular weight biopolymers

410 such as polysaccharides and proteins. These phytoplankton-derived substrates fuel heterotrophs, including the heterotrophic bacteria that cycle a large fraction of marine productivity (Azam and Malfatti, 2007). The nature and structure of the phytoplankton-derived biopolymers also dictate the enzymatic tools needed by heterotrophic microbial communities to access them (Gugi et al., 2015; Thomas et al., 2017). Microbial communities vary in their summed genetic capabilities and the extent to which they can activate them at a specific time and place; thus, substrates that are labile in one location may be recalcitrant

415 in another (Arnosti et al., 2021). Untangling these interrelationships—the structure of the biopolymers, the composition and capabilities of the heterotrophic communities, and the activities of the specific enzymes they produce—is essential to understand the rate and location at which organic matter is cycled in the ocean.

4.1 Depth- and site-related patterns in carbohydrate epitopes, microbial communities, and their enzymatic capabilities

Carbohydrate epitopes—and therefore the structural complexity of intact polysaccharides—differed considerably by

420 location, despite similarities in their monosaccharide constituents (Figs. 2-3). Previous investigations have demonstrated depth differences but not location-related differences in monosaccharide constituents of POM (Aluwihare et al., 1997). Our monosaccharide data also show this pattern, but the carbohydrate epitopes show a more refined picture. For example, at Stn. 19—where chlorophyll concentrations were highest—we found the broadest array of epitopes in surface and DCM waters: seven different types in all, including two that were evident only in the NaOH extract. In contrast, at Stn. 18, in the Gulf

425 Stream, we detected just two epitopes in surface and DCM waters (Fig. 3). The differences in polysaccharide complexity at these stations could be in part driven by the different phytoplankton communities that dominate in distinct regions of the western North Atlantic (Bolaños et al., 2020; Della Penna and Gaube, 2019). Thus, the similarities in 'building blocks' of polysaccharides mask the differences in the structures from which they are derived (Fig. 9).
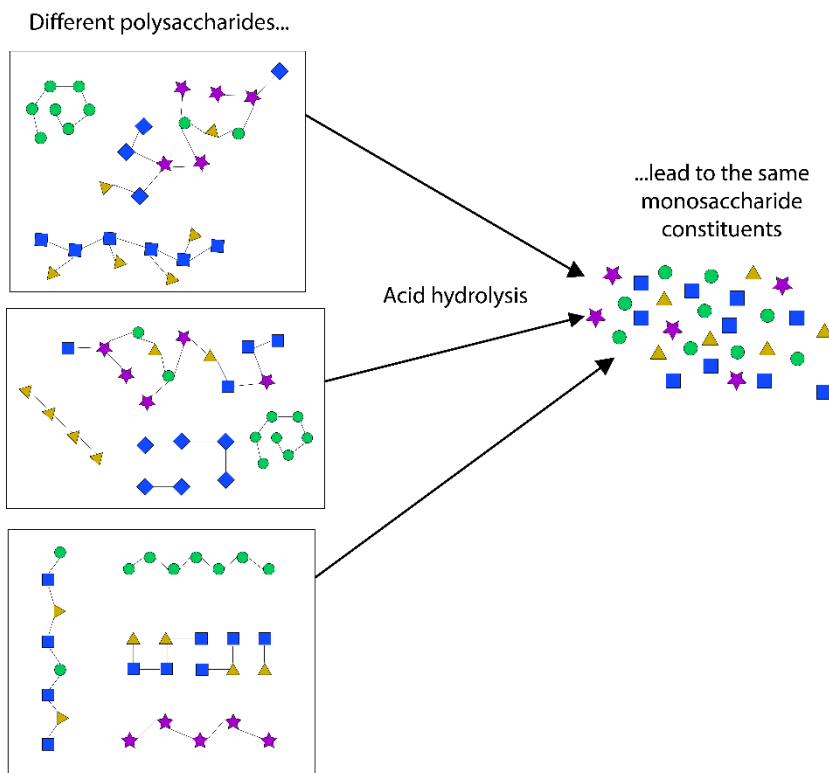
430 **Figure 9: As shown conceptually in this figure, the structural complexity of polysaccharides differs by station, despite the monosaccharide constituents of combined carbohydrates being indistinguishable between stations.**

In accordance with the structural differences indicated by carbohydrate epitopes, activities of extracellular enzymes—which are also very sensitive to substrate structural features—differed notably by station and depth (Fig. 6). To distinguish between potential activities for polysaccharides and proteins, the two key components of marine organic matter (Hedges et al.,

435 2002), we measured a series of substrates that vary in structural complexity as well as enzyme class. Polysaccharide hydrolase activities show spatial variations that parallel differences in microbial community composition (Arnosti et al., 2011; 2012); depth-related patterns have also been observed (Steen et al., 2012; Hoarfrost and Arnosti 2017; Balmonte et al., 2021; Lloyd et al., 2023). Glucosidase and peptidase activities were also distinct among stations but did not show the same connections with the microbial communities (Figs. 4,5; Suppl. Fig. 3). Here, we also examined the statistical connection among

440 polysaccharide- and protein-hydrolyzing enzymes. Among the four stations, a handful of very robust correlations in enzyme activities were evident (Fig. 7), but there were also considerable differences among individual stations (Fig. S6). These variations in activities likely reflect the considerable variety of enzymes produced even by closely related bacteria (Avci et al., 2020, Krüger et al., 2019), as well as resource prioritization for specific substrates among bacteria (Koch et al., 2019).

445

Given the depth stratification of microbial communities (Fig. 4b), which extends to the ability of communities to excrete extracellular enzymes (Zhao et al., 2020), we also constructed a corrplot focusing on enzyme activities by depth zone (Fig. 8), which revealed patterns not evident from the depth-integrated corrplots (Fig. 7). Most notably, in the mesopelagic, virtually all of the polysaccharide hydrolases correlate with one another, despite the fact that distinctly different enzymes are

450   responsible for hydrolysis of these polysaccharides (e.g., Becker et al., 2020; Reisky et al., 2019; Sichert et al., 2020). Moreover, in the mesopelagic β-glucosidase activities also positively correlated with all the polysaccharide hydrolase activities, a pattern not seen in other depth zones, or in the depth-integrated corrplots. Peptidase correlations, however, were not notably more prevalent in the mesopelagic than in other depth zones. These correlations suggest that in the mesopelagic, polysaccharides—including those with more complex structures—are a specific target, in accordance with studies that have

455   demonstrated intense organic matter remineralization in this zone (Boyd et al., 1999; Buesseler et al., 2007).

One somewhat surprising observation is that activities of the exo-acting enzymes (β- and α-glucosidase, leucine aminopeptidase) seldom showed positive correlations with endo-acting enzymes targeting the same substrate class. Moreover, α- and β-glucosidase activities did not generally show positive correlations with each other; only in the mesopelagic did β-

460   glucosidase (but not α-glucosidase) consistently correlate with polysaccharide hydrolase activities. Leucine aminopeptidase activity overall strongly correlated with the monomers of combined carbohydrates (Fig 7), perhaps a sign of activity hydrolyzing terminal amino acids from polysaccharide structures, given that leucine aminopeptidase activity integrates the activities of multiple exo-acting peptidases (Steen et al., 2015). However, leucine-aminopeptidase activities did not otherwise show broad-scale correlations with the endopeptidase activities. The lack of correlations between the exo- and endo-acting

465   enzymes targeting carbohydrates, as well as those targeting peptides, therefore suggest that the exo-activities should not be used as overall proxies for polysaccharide or protein degradation by microbial communities.

Spatial differences in enzyme activities are likely a function of depth- and location-related differences in microbial community composition (Fig. 5). These differences have been linked to substrate availability, as in the case of the shifting

470   nature of organic matter produced during phytoplankton blooms (e.g. Teeling et al., 2012; Dlugosch et al., 2023), with specific organisms targeting distinct polysaccharide structures (Francis et al., 2021; Giljan et al., 2023; Orellana et al., 2022). While depth-stratification in microbial composition has been previously reported (e.g., DeLong et al., 2006), also for the northwestern Atlantic Ocean (Zorz et al., 2019), we also found differences in community composition by location (Fig 4). Location-related differences were especially pronounced in the surface ocean (Fig. 4), where physical, biological, and chemical properties of

475   the water masses differed considerably (Fig. 1; Table 1). However, bacterial communities in the deep ocean also differed across stations, although the water below 1500 m from all stations had characteristics typical of North Atlantic Deep Water (Broecker, 1991; Figs. 1, 4). These differences in the deep ocean could be due in part to the ca. 2000 m difference in bottom water depths between Stns. 18 and 20 (Table 1), as well as from differences in the quantity and nature of sinking particles at each location

(Mestre et al., 2018; Pelve et al., 2017), which may also affect enzymatic activities in the deep ocean (Lloyd et al., 2022). At
480 all stations and depths, however, we find organisms—including members of the Bacteroidota and Gammaproteobacteria—that
typically are well-equipped to decompose biopolymers (Fig. 5; Buchan et al., 2014; Francis et al., 2021).

4.2 Polysaccharide structural complexity could in part explain patterns of heterotrophic carbon cycling in the ocean

This analysis of carbohydrate epitopes in POM, among the first results from open ocean samples (Priest et al., 2023),
provides insight into the composition of intact polysaccharides in the upper ocean. The presence of 1,3-β-D-glycans and
485 alginate at all stations in surface and DCM waters (Fig. 3) demonstrates that laminarin and alginate-derived structures are
found in POM from a broad range of locations. At Stns. 17, 19, and 20, moreover, at least one of the fucoidan epitopes was
detected in POM from surface waters. Detection of these structures is particularly intriguing, since laminarin and fucoidan in
essence are at the opposite ends of the degradation spectrum. Laminarin is rapidly hydrolyzed in most ocean waters, but
fucoidan hydrolysis is rarely detected in the water column (Arnosti et al., 2011; Hoarfrost and Arnosti, 2017; Balmonte et al.,
490 2021; Lloyd et al., 2023). This pattern holds for the current investigation as well, where fucoidan hydrolysis was only
measurable at 300 m at Stns. 18 and 20, whereas laminarin hydrolysis was widely detected, at 19 of the 23 stations and depths
(Fig. 5).

The difference in hydrolysis of laminarin and fucoidan is likely linked to substrate structural complexity, since the
495 number of different types of enzymes required to hydrolyze a polysaccharide scales linearly with polysaccharide structural
complexity (Bligh et al., 2022); fucoidan in particular represents a hydrolytic challenge (Sichert et al., 2020). POM in the upper
ocean may therefore include polysaccharide structures that are highly labile, as well as those that are generally recalcitrant
with respect to bacterial remineralization. We surmise that with increasing depth in the ocean, the contribution of labile
constituents would decrease, and the relative contribution of recalcitrant polysaccharides would be enhanced. Testing this
500 hypothesis would require investigation of polysaccharide epitopes in POM collected in deep water, where sinking particles
can be substantially re-worked by bacterial communities. In the current investigation, however, aside from the (shallow)
bottom water at Stn. 17, we were not able to detect polysaccharide epitopes in POM from the deep ocean. Given the low
concentrations of POM in the deep ocean (Table 1; Baker et al., 2017), the potential for incomplete extraction of
polysaccharides by our methods, and the comparatively small volume of water we filtered for POM analysis, we surmise that
505 any polysaccharides present in deeper samples were below our limit of detection. Alternatively, deep ocean POM may not be
characterizable using epitopes due to bacterial transformations of sinking particles (Wakeham et al., 1997; Hedges et al., 2001;
Kharbusch et al., 2020). However, previous studies have also reported rapid fluxes of fresh organic matter to the deep ocean
(Ruiz-Gonzalez et al., 2020; Poff et al., 2021), suggesting that labile polysaccharides may be present even in deep waters. In
support of this point, bathypelagic bacteria capable of selfish uptake of a broad range of polysaccharides (including fucoidan)
510 have recently been identified in deep ocean waters, suggesting that intact polysaccharides are components of this fresh organic

24

matter that reaches the bottom of the ocean (Giljan et al., 2023). Collection of larger quantities of POM, and/or improvements in extraction methods, may lead in the future to characterization of intact polysaccharides in deep ocean POM.

Conclusions

The structural complexity of polysaccharides thus could help explain some of the patterns of the enzymatic
515 capabilities of microbial communities and the *in-situ* carbohydrate signatures we observe, information that is not evident when analyzing the individual monosaccharide building blocks of combined carbohydrates (Fig. 9). Specifically, spatial variability in polysaccharide structures in surface waters could help explain the variability in polysaccharide hydrolase activities between the four stations (Figs. 3,6); this variability may not exist to the same extent in the peptidase activities (Fig. 5), since peptidases have a broader array of target substrates (Lapébie et al., 2019). Comparing polysaccharide epitopes with the polysaccharide
520 hydrolase activities begins to reveal the intricacies of the microbial community's enzymatic toolbox and how these activities vary with space and depth in the ocean. Further assessment of polysaccharide structural complexity in the deep ocean—and comparing to the enzymatic capabilities of bacterial communities—may begin to help answer questions focused on why organic carbon persists under varying environmental conditions.

Competing Interests

525 The contact author has declared that none of the authors has any competing interests.

Author Contributions

C. Lloyd: Investigation, Formal analysis, Data curation, Visualization, Writing – Original Draft, Writing – Review and Editing; **S. Brown:** Investigation, Data curation, Methodology, Writing – Original Draft; Writing – Review and Editing; **G. Giljan:** Investigation, Data curation, Visualization, Investigation, Writing – Original Draft; Writing – Review and Editing; **S.**
535 **Vidal-Melgosa:** Data curation, Methodology, Investigation, Writing – Review and Editing; **N. Steinke:** Investigation, Writing – Review and Editing; **S. Ghobrial:** Methodology, Investigation, Writing – Review and Editing; **R. Amann:** Investigation,

Writing – Review and Editing, Supervision, Funding acquisition; **C. Arnosti:** Conceptualization, Methodology, Investigation, Writing – Original Draft, Writing – Review and Editing, Supervision, Project administration, Funding acquisition

540

References

Aluwihare, L., Repeta, D., and Chen, F.: A major biopolymeric component to dissolved organic carbon in surface sea water, Nature, 387, 166-169, 1997.

545 Andres, M., Muglia, M., Bahr, F., Bane, J.: Continuous Flow of Upper Labrador Sea Water around Cape Hatteras, Sci. Rep., 8(1), 4494, doi: 10.1038/s41598-018-22758-z, 2018.

Arnosti, C.: Fluorescent derivatization of polysaccharides and carbohydrate-containing biopolymers for measurement of enzyme activities in complex media, J. Chromatogr. B. Analyt. Technol. Biomed. Life Sci., 793, 181-191, doi: 550 10.1016/s1570-0232(03)00375-1, 2003.

Arnosti, C.: Microbial extracellular enzymes and the marine carbon cycle, Ann. Rev. Mar. Sci., 3, 401–425, doi: 10.1146/annurev-marine-120709-14273, 2011.

555 Arnosti, C., Steen, A.D., Ziervogel, K., Ghobrial, S., Jeffrey, W.H.: Latitudinal gradients in degradation of marine dissolved organic carbon, PLoS ONE, 6(12), e28900, doi: 10.1371/journal.pone.0028900, 2011.

Arnosti, C., Fuchs, B., Amann, R., Passow, U.: Contrasting extracellular enzyme activities of particle associated bacteria from distinct provinces of the North Atlantic Ocean, Front. Microbiol., 3, 425, 2012.
560
Arnosti, C., Wietz, M., Brinkhoff, T., Hehemann, J.-H., Probandt, D., Zeugner, L., Amann, R.: The biogeochemistry of marine polysaccharides: Sources, inventories, and bacterial drivers of the carbohydrate cycle, Annual Review of Marine Science, 13, doi: 10.1146/annurev-marine-032020-012810, 2021.

565 Avci, B., Kruger, K., Fuchs, B.M., Teeling, H., and Amann, R.I.: Polysaccharide niche partitioning of distinct Polaribacter clades during North Sea spring algal blooms, The ISME J., 14, 1369-1383, 2020.

Azam, F., and Malfatti, F.: Microbial structuring of marine ecosystems, Nat. Rev. Microbiol., 5, 782–791, doi:10.1038/nmicro1747, 2007.

570

Baker, C.A., Henson, S.A., Cavan, E.L., Giering, S.L.C., Yool, A., Gehlen, M., Belcher, A., Riley, J.S., Smith, H.E.K., Sanders, R.: Slow-sinking particulate organic carbon in the Atlantic Ocean: Magnitude, flux, and potential controls, Global Biogeochem. Cycles, 31(7), 105101065, doi: 10.1002/2017GB005638, 2017.

575 Balmonte, J.P., Teske, A., Arnosti, C.: Structure and function of high Arctic pelagic, particle-associated and benthic bacterial communities, Environ. Microbiol., 20, 2941-2959, 2018.

Balmonte, J.P., Simon, M., Giebel, H.-A., Arnosti, C.: A sea change in microbial enzymes: Heterogeneous latitudinal and depth-related gradients in bulk water and particle-associated enzymatic activities from 30°S to 59°N in the Pacific
580 Ocean, Limnol. Ocean., 66, 3489-3507, doi: 10.1002/lno.11894, 2021.

Becker, S., Scheffel, A., Polz, M., Hehemann, J-H.: Accurate quantification of laminarin in marine organic matter with enzymes from marine microbes, Appl. Environ. Microbiol., 83, e03389-16, 2017.

585 Becker, S., Tebben, J., Coffinet, S., Hehemann, J.-H.: Laminarin is a major molecule in the marine carbon cycle, PNAS, 117(12), 6599-6607, doi:10.1073/pnas.1917001117, 2020.

Bennke, C.M., Reintjes, G., Schattenhofer, M., Ellrott, A., Wulf, J., Zeder, M., Fuchs, B.M.: Modification of a high-throughput automatic microbial cell enumeration system for shipboard analyses, Appl. Environ. Microbiol., 82,
590 3289-3296, 2016.

Bligh, M., Nguyen, N., Buck-Wiese, H., Vidal-Melgosa, S., Hehemann, J.-H.: Structures and functions of algal glycans shape their capacity to sequester carbon in the ocean, Curr Opin Chem Biol., 71, 102204, doi: 10.1016/j.cbpa.2022.102204, 2022.

595

Bolaños, L., Karp-Boss, L., Choi, C., Worden, A., Graff, J., Haentjens, N., Chase, A., Penna, A., Gaube, P., Morison, F., Menden-Deuer, S., Westberry, T., O'Malley, R., Boss, E., Behrenfeld, M., Giovannoni, S.: Small phytoplankton dominate western North Atlantic biomass, The ISME J., 14, 1663-1674, doi: 10.1038/s41396-020-0636-0, 2020.

600 Broecker, W.: The great ocean conveyor, Oceanography, 4(2), 79–89, doi: 10.5670/oceanog.1991.07, 1991.

Buck-Wiese, H., Andskog, M.A., Nguyen, N.P., Asmala, E., Vidal-Melgosa, S., Liebke, M., Gustafsson, C., Hehemann, J.-H.: Fucoid brown algae inject fucoidan carbon into the ocean, PNAS, 120(1), e2210561119, doi: 10.1073/pnas.2210561119, 2023.

605

Buesseler, K.O., Lamborg, C.H., Boyd, P.W., Lam, P.J., Trull, T.W., Bidigare, R.R., Bishop, J.K., Casciotti, K.L., Dehairs, F., Elskens, M., Honda, M., Karl, D.M., Siegel, D.A., Silver, M.W., Steinberg, D.K., Valdes, J., Van Mooy, B., Wilson, S.: Revisiting carbon flux through the ocean's twilight zone, Science, 316(5824), 567-570, 2007.

610   Bushnell, B.: BBTools software package, 578, http://sourceforge. net/projects/bbmap, 2014.

Della Penna, A., and Gaube, P.: Overview of (Sub)mesoscale ocean dynamics for the NAAMES field program, Frontiers Mar. Sci., 6, 384, 2019.

615   Engel, A., Handel, B.: A novel protocol for determining the concentration and composition of sugars in particulate and in high molecular weight dissolved organic matter (HMW-DOM) in seawater, Mar. Chem., 127, 180-191, doi: 10.1016/j.marchem.2011.09.004, 2011.

Francis, B.T., Bartosik, D., Sura, T., Sichert, A., Hehemann, J.-H., Markert, S., Schweder, T., Fuchs, B.M., Teeling, H.,
620   Amann, R.I., Becher, D.: Changing expression of TonB-dependent transporters suggest shifts in polysaccharide consumption over the course of a spring phytoplankton bloom, The ISME J., 15, 2336-2350, doi: 10.1038/s41396-021-00928-8, 2021.

Fratantoni, P.S., and Pickart, R.S.: The western North Atlantic shelfbreak current system in summer, Journal of Physical
625   Oceanography, 37(10), 2509-2533, 2007.

Giljan, G., Brown, S., Lloyd, C.C., Ghobrial, S., Amann, R., Arnosti, C.: Selfish bacteria are active throughout the water column of the ocean, ISME Commun., 3(1), 11, doi: 10.1038/s43705-023-00219-7, 2023.

630   Hedges, J.I., Eglinton, G., Hatcher, P.G., Kirchman, D.L., Arnosti, C., Derenne, S., Evershed, R.P., Kogel-Knaber, I., de Leeuw, J.W., Littke, R., Michaelis, W., Rullkotter, J.: The molecularly-uncharacterized component of nonliving organic matter in natural environments, Org Geochem., 31(10), 945-958, doi: 10.1016/S0146-6380(00)00096-6, 2000.

Hedges, J.I., Baldock, J.A., Gelinas, Y., Lee, C., Peterson, M., Wakeham, S.G.: Evidence for non-selective preservation of
635   organic matter in sinking marine particles, Nature, 409, 801-804, 2001.

Hedges, J.I., Baldock, J.A., Gelinas, Y., Lee, C., Peterson, M., Wakeham, S.G.: The biochemical and elemental compositions of marine plankton: a NMR perspective, Mar. Chem., 78, 47-63, 2002.

640 Heidrich, J., and Todd, R.E.: Along-stream evolution of Gulf Stream volume transport, Journal of Phys. Oceanogr., 50(8), 2251-2270, doi: 10.1175/JPO-D-0303.1, 2020.

Herlemann, D.P.R., Labrenz, M., Jürgens, K., Bertilsson, S., Waniek, J.J., Andersson, A.F.: Transitions in bacterial communities along the 2000 km salinity gradient of the Baltic Sea, The ISME J., 5, 1571–1579, 2011.

645

Hoarfrost, A., and Arnosti, C.: Heterotrophic extracellular enzymatic activities in the atlantic ocean follow patterns across spatial and depth regimes, Front. Mar. Sci., 4, 200, doi: 10.3389/fmars.2017.00200, 2017.

Kharbush, J., Close, H., Van Mooy, B., Arnosti, C., Smittenberg, R., Le Moigne, F., Molienhauer, G., Scholz-Bottcher, B., 650 Obreht, I., Koch, B., Becker, K., Iversen, M., Mohr, W.: Particulate Organic Carbon Deconstructed: Molecular and Chemical Composition of Particulate Organic Carbon in the Ocean, Front. Mar. Sci., 7, 00518, doi: 10.3389/fmars.2020.00518, 2020.

Kirchman, D. L.: Measuring bacterial biomass production and growth rates from leucine incorporation in natural aquatic 655 environments, Methods Microbiol., 30, 227–237, doi: 10.1016/s0580-9517(01)30047-8, 2001.

Koch, H., Dürwald, A., Schweder, T., Noriega-Ortega, B., Vidal-Melgosa, S., Hehemann, J.-H., Dittmar, T., Freese, H.M., Becher D., Simon, M., Wietz, M.: Biphasic cellular adaptations and ecological imlplications of Alteromonas macleodii degrading a mixture of algal polysaccharides, The ISME J., 13, 92-103, doi: 10.1038/s41396-018-0252-4, 2019.

660

Krüger, K., Chafee, M., Francis, T.B., Glavina del Rio, T., Becher, D., Schweder, T., Amann, R.I., Teeling, H.: In marine Bacteroidetes the bulk of glycan degradation during algae blooms is mediated by few clades using a restricted set of genes, The ISME J., 13, 2800–16, 2019.

665 Laine, R.A.: A calculation of all possible oligosaccharide isomers both branched and linear yields 1.05×10^{12} structures for a reducing hexasaccharide: the Isomer Barrier to development of single-method saccharide sequencing or synthesis systems, Glycobiology, 4(6), 759-767, doi: 10.1093/glycob/4.6.759, 1994.

29

Lapébie, P., Lombard, V., Drula, E., Terrapon, N., Henrissat, B.: Bacteroidetes use thousands of enzyme combinations to break
670   down glycans, Nature Comm., 10, 2043, 2019.

Liu, M., and Tanhua, T.: Water masses in the Atlantic Ocean: characteristics and distributions, Ocean Sci., 17, 463-486, doi:
       10.5194/os-17-463-2021, 2021.

675 Lombard, V., Ramulu, H.G., Drula, E., Coutinho, P.M., Henrissat. B.: The carbohydrate-active enzymes database (CAZy) in
       2013, Nucleic Acids Res., 42, D490-495, doi: 10.1093/mar/gkt1178, 2014.

Mestre, M., Ruiz-González, C., Logares, R., Duarte, C.M., Gasol, J.M., Sala, M.M.: Sinking particles promote vertical
       connectivity in the ocean microbiome. PNAS, 115(29), E6799–E6807, doi: 10.1073/pnas.1802470115, 2018.

680
Morris, R.M., Nunn, B.L., Frazar, C., Goodlett, D.R., Ting, Y.S., Rocap, G.: Comparative metaproteomics reveals ocean-scale
       shifts in microbial nutrient utilization and energy transduction, The ISME J, 5, 673-685, 2010.

Pelve, E., Fontanez, K., DeLong, E.: Bacterial Succession on Sinking Particles in the Ocean's Interior, Front. Microbiol., 8,
685   2269, doi: 10.3389/fmicb.2017.02269, 2017.

Poff, D.E., Leu, A.O., Eppley, J.M., Karl, D.M., DeLong, E.F.: Microbial dynamics of elevated carbon flux in the open ocean's
       abyss, PNAS, 118, e2018269118, doi: 10.1073/pnas.2018269118, 2021.

690 Priest, T., Vidal-Melgosa, S., Hehemann, J.-H., Aman, R., Fuchs, B.M.: Carbohydrates and carbohydrate degradation gene
       abundance and transcription in Atlantic waters of the Arctic, ISME Comm., 3, 130, doi: 10.1038/s43705-023-00324-
       7, 2023.

Quast, C., Pruesse, E., Yilmaz, P., Gerken, J., Schweer, T., Yarza, P., Peplies, J., Glöckner, F.O.: The SILVA ribosomal RNA
695   gene database project: improved data processing and web-based tools, Nuc. Acids Res., 41, 590–596, 2013.

Reisky, L., Prechoux, A., Zuhlke, M.-K., Baumgen, M., Robb, C.S., Gerlach, N., Roret, T., Stanetty, C., Larocque, R., Michel,
       G., Song, T., Markert, S., Unfried, F., Mihovilovic, M.D., Trautwein-Schult, A., Becher, D., Schweder, T.,
       Bornscheuer, U.T., Hehemann, J.-H.: A marine bacterial enzymatic cascade degrades the algal polysaccharide ulvan,
700   Nat. Chem. Biol., 15, 803-812, 2019.

Ruiz-González, C., Mestre, M., Estrada, M., Sebastián, M., Salazar, G., Agustí, S., Moreno-Ostos, E., Reche, I., Álvarez-Salgado, X.A., Morán, X.A.G., Duarte, C.M., Sala, M.M., Gasol, J.M.: Major imprint of surface plankton on deep ocean prokaryotic structure and activity, Mol. Ecol., 29, 1820–1838, doi: 10.1111/mec.15454, 2020.

705

Saito, M.A., Bertrand, E.M., Duffy, M.E., Gaylord, D.A., Held, N.A., Hervey IV, W.J., Hettich, R.L., Jagtap, P.D., Janech, M.G., Kinkade, D.B., Leary, D.H., McIlvin, M.R., Moore, E.K., Morris, R.M., Neely, B.A., Nunn, B.L., Saunders, J.K., Shepherd, A.I., Symmonds, N.I., Walsh, D.A.: Progress and challenges in ocean metaproteomics and proposed best practices for data sharing, Journal of Proteome Research, 18, 1461-1476, 2019.

710

Sichert, A., Corzett, C. H., Schechter, M. S., Unfried, F., Markert, S., Becher, D., Fernandez-Guerra, A., Liebeke, M., Schweder, T., Polz, M. F., Hehemann, J.-H.: Verrucomicrobia use hundreds of enzymes to digest the algal polysaccharide fucoidan, Nature Comm., 5, 1026-1039, 2020.

715 Simon, M. and Azam, F.: Protein content and protein synthesis rates of planktonic marine bacteria, Mar. Ecol. Prog. Ser., 51, 201–213, 1989.

Steen, A.D., Ziervogel, K., Ghobrial, S., Arnosti, C.: Functional variation among polysaccharide-hydrolyzing microbial communities in the Gulf of Mexico, Mar. Chem., 138-139, 13-20, doi: 10.1016/j.marchem/2012.06.001, 2012.

720

Steen, A.D., Vazin, J.P., Hagen, S.M., Mulligan, K.H., Wilhelm, S.W.: Substrate specificity of aquatic extracellular peptidases assessed by competitive inhibition assays using synthetic substrates, Aquat. Microb. Ecol., 75, 271-281, doi: 10.3354/ame01175, 2015.

725 Teeling, H., Fuchs, B.M., Becher, D., Klockow, C., Gardebrecht, A., Bennke, C.M., Kassagby, M., Huang, S., Mann, A.J., Waldmann, J., Weber, M., Klindworth, A., Otto, A., Lange, J., Bernhardt, J., Reinsch, C., Hecker, M., Peplies, J., Bockelmann, F.D., Callies, U., Gerdts, G., Wichels, A., Wiltshire, K.H., Glöckner, F.O., Schweder, T., Amann, R.: Substrate-controlled succession of marine bacterioplankton populations induced by a phytoplankton bloom, Science, 336, 608-611, 2012.

730

Vidal-Melgosa, S., Sichert, A., Francis, T., Bartosik, D., Niggemann, J., Wichels, A., Willats, W., Fuchs, B., Teeling, H., Becher, D., Schweder, T., Amann, R., Hehemann, J.-H.: Diatom fucan polysaccharide precipitates carbon during algal blooms, Nature Comm., 12, 1150, doi: 10.1038/s41467-021-21009-6, 2021.

735 Wakeham, S.G., Lee, C., Hedges, J.I., Hernes, P.J., Peterson, M.L.: Molecular indicators of diagenetic status in marine organic
matter, Geochim. Cosmochim. Acta, 61, 5363–5369, doi: 10.1016/S0016-7037(97)00312-8, 1997.

Zorz, J., Willis, C., Comeau, A.M., Langille, M.G.I., Johnson, C.L., Li, W.K.W., LaRoche, J.: Drivers of Regional Bacterial
Community Structure and Diversity in the Northwest Atlantic Ocean, Front Microbiol., 10, 00281, doi:
740 10.3389/fmicb.2019.00281, 2019.

Table 1. Volume of water filtered (L) for POM analyses.

Depths	Stn 17	Stn 18	Stn 19	Stn 20
Surface	6.0	9.5	5.0	13.5
DCM	5.5	8.5	5.5	12.5
300 m	-	13.5	15.0	14.5
OMZ	9.0	11.0	14.5	12.5
1500 m	-	14.0	14.0	15.0
3000 m	-	-	13.7	13.5
Bottom	-	13.5	12.5	13.0

745 **Table 2.** Environmental parameters of sampling site.

Stn	Depth	Depth (m)	T (°C)	S (psu)	Oxygen (ml/L)	Chlorophyll-a (mg/m^3)	POC (mg/L)	Cell Counts (Cells/mL)
17	1	2	25.0	36.39	4.61	0.118	0.0353	6.84E05
17	2	64	22.9	36.45	4.54	0.690	0.0511	4.28E05
17	3	625	5.6	35.04	4.92	0.111	0.0187	8.97E04
18	1	2	25.2	36.42	4.48	0.147	0.0203	4.00E05
18	2	104	23.4	36.67	4.53	0.401	0.0204	3.55E05
18	3	300	18.8	36.61	4.30	0.070	0.00096	1.43E05
18	4	800	9.2	35.21	3.18	0.079	0.00326	3.83E04
18	5	1500	4.4	34.99	5.63	0.088	0.00573	2.60E04
18	6	3190	2.3	34.89	5.89	0.116	0.00859	2.42E04
19	1	2	8.8	33.72	6.63	1.49	0.160	9.71E05
19	2	33	9.3	33.94	6.45	1.32	0.136	1.62E06
19	3	300	9.9	35.21	3.36	0.110	0.0106	1.44E05
19	4	850	5.1	35.03	5.32	0.102	0.00599	2.38E04
19	5	1500	3.9	34.94	5.89	0.093	0.00582	1.62E04
19	6	3000	2.8	34.92	5.90	0.044	0	2.18E04
19	7	4325	2.2	34.88	5.73	0.082	0.00852	2.08E04
20	1	2	21.0	36.73	4.92	0.110	0.0253	3.66E05
20	2	64	20.1	36.68	5.03	0.212	0.0253	4.29E05
20	3	300	18.3	36.56	4.69	0.019	0.00306	2.45E05

20	4	800	10.1	35.33	3.46	0.00	0.00900	5.35E04
20	5	1500	4.6	35.01	5.54	0.00	0.00147	2.23E04
20	6	3000	3.0	34.93	5.66	0.058	0.00057	1.12E04
20	7	5580	2.2	34.85	5.46	0.0087	0.00242	9.67E03